23rd ABCM International Congress of Mechanical Engineering
December 6-11, 2015, Rio de Janeiro, RJ, Brazil

NONLINEAR VIBRATION EFFECTS DURING INDUCTION MOTOR ACCELERATION

Marcio Coelho de Mattos
Wenderson Luiz Ganda
Universidade Federal do Espírito Santo, Departamento de Engenharia Mecânica. Av. Fernando Ferrari, 514, Caixa Postal 9011, Goiabeiras. CEP 29075-910, Vitória-ES, Brasil.
marcio.mattos@ufes.br, wlganda@petrobras.com.br

Abstract. *This article presents a study on nonlinear vibration effects that can occur during induction motor acceleration, due to an interaction between motor and elastic support structure dynamics. A coupled model was obtained and subsequently simulated to verify whether nonlinear effects, like Sommerfeld or Chaos effect, can occur.*

Keywords: *Nonlinear dynamical systems, Induction motor, Vibrations, Nonlinear Oscillations.*

1. INTRODUCTION

Vibration analysis in electromechanical systems is very important because most of motor drives experiment vibration problems due to inherent unbalance, as a result of failure in project, maintenance or installation. In addition, not only the equipment can fail, but also the structure, components or support bases. Furthermore, vibration can cause faster friction in machine parts, like bearings, gears, screws, couplings and fixation elements when the machine natural frequency matches the excitation frequency. In this situation, a phenomenon called resonance occurs, possibly leading to excessive deflection or destructive failures (Rao, 2013).

Motor vibration analysis itself is widely known, and monitoring and prediction techniques are usual in industry. However, it is also important to analyze the interaction between motor and its support base. There are some nonlinear oscillations that can occur in these coupled systems, and its effects have been studied for systems formed by direct current motor (DC motor) and an elastic base, as can be seen in Balthazar *et al*. (2003) and Rocha (2004). Nevertheless, DC motor has no longer been used in large scale in industrial processes. In recent years, drives based on DC motors have been gradually substituted by drives based on Alternate Current Three-phase Induction Motor (TIM).

The objective of this study is to analyze and simulate systems composed of elastic base support and TIM using coupled dynamic models, in order to identify and verify whether nonlinear oscillation phenomena are relevant to this motor type.

2. NONLINEAR VIBRATION IN ELETROMECHANICAL SYSTEMS

Non-ideal systems composed of an electrical motor and an elastic base were analyzed by Sommerfeld in the early 1900s. He observed that, in resonance region, DC motor rotation had not varied linearly along with armor voltage. In other words, when voltage increased, rotation had not increased linearly. Thus, the energy injected in the systems was consumed in order to increase the vibration amplitude. It seemed that the motor was captured by the resonance. After some energy amount had been injected, a jump occurred and the rotation returned to vary linearly, along with voltage. This effect was known as Sommerfeld effect and was studied in many arrangements with DC motors (Balthazar *et al*.,2003).

Other nonlinear effect type that can occur in systems like this is the Chaos. It occurs when a small variation or disturbance in the system entry provokes a large variation in exit parameters. Discussion about this and other oscillations nonlinear effects can be obtained in Strogatz *et al.*, (1994).

Although TIM is nowadays the most important motor drive in industry, there are just a few studies about systems composed of TIM and an elastic base. A system with a synchronous motor starting, like an induction motor, was analyzed by Leonov (2008), but with a very simplified motor dynamic model that has not regarded motor electrical dynamics, showing that, in direct starts, Sommerfeld effect cannot occur. Other example is shown in Zucovic and Cveticanin (2009), also with a TIM simplified model, showing that, with nonlinear base coil, the effect can occur.

3. ELECTROMECHANICAL DYNAMIC MODEL

The system that will be investigated physical model is shown in Fig.1.

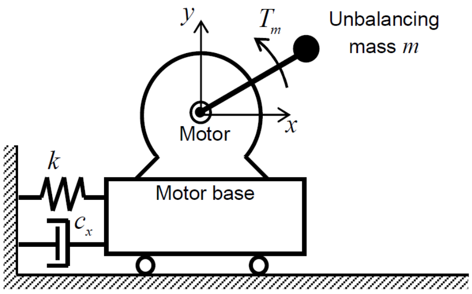

Figure 1. Induction motor with unbalanced rotor and its elastic support.

In this system, TIM has M mass, and rotor unbalancing can be represented by $m.r$, where r is radius in which the unbalancing mass is localized. The c_θ is the angular viscous damping coefficient and J is the rotor inertia moment. Elastic support stiffness is k and c_x is the viscous damping coefficient. Rotor angular displacement is θ and motor linear displacement is x.

3.1 Mechanical Model

In order to obtain the mechanical movement equations, Lagrange's equation can be used, with kinetic energy as T and potential energy as V, with $L = T - V$. So, Lagrange's equation can be written as:

$$\frac{\partial L}{\partial t}\left(\frac{\partial L}{\partial \dot{q}_i}\right) - \frac{\partial L}{\partial q_i} = Q_i \tag{1}$$

Where qi is motion generalized coordinate and Qi is the qi coordinate acting generalized force.

The system kinetic and potential energy can be expressed as:

$$T = \frac{M\dot{x}^2}{2} + \frac{mv^2}{2} + \frac{J\dot{\theta}^2}{2} \tag{2}$$

$$V = \frac{kx^2}{2} + mgr(1 + \sin(\theta)) \tag{3}$$

Where $v^2 = v^2_x + v^2_y$. So, Eq. (2) can be rewritten as:

$$T = \frac{(M+m)\dot{x}^2}{2} - mr\dot{x}\dot{\theta}\sin(\theta) + \frac{mr^2\dot{\theta}^2}{2} + \frac{J\dot{\theta}^2}{2} \tag{4}$$

Applying Eq. (1) for x and θ coordinates using Eq. (3) and Eq. (4), the system governing equations are:

$$(M+m)\ddot{x} + c_x\dot{x} + kx - mr\ddot{\theta}\sin(\theta) - mr\dot{\theta}^2\cos(\theta) = 0 \tag{5}$$

$$(J + mr^2)\ddot{\theta} + c_\theta\dot{\theta} - mr\ddot{x}\sin(\theta) + mgr\cos(\theta) = T_e - T_L \tag{6}$$

Where T_e is the motor torque and T_L is the load torque. In order to write the equations taking into account as many dimensionless parameters as possible, one defines:

$$\zeta_x = \frac{c_x}{(M+m)} \quad \omega_0 = \sqrt{\frac{k}{(M+m)}}$$
$$\mu = \frac{mr}{(M+m)} \quad \zeta_\theta = \frac{c_\theta}{(J+mr^2)} \tag{7}$$
$$\varepsilon = \frac{mr}{(J+mr^2)} \quad \alpha = \frac{1}{(J+mr^2)}$$

Taking the relations from Eq. (7) into account in Eq. (5) and Eq. (6), the system governing equations can be written in the following form:

$$\ddot{x} = -\zeta_x \dot{x} - \omega_0^2 x + \mu\ddot{\theta}\sin(\theta) + \mu\dot{\theta}^2\cos(\theta) \tag{8}$$

$$\ddot{\theta} = -\zeta_\theta \dot{\theta} + \varepsilon \ddot{x}\sin(\theta) - \varepsilon g\cos(\theta) + \alpha\left(T_e - T_L\right) \tag{9}$$

3.2 Electric Motor Dynamic Equations

The motor dynamic electric model is necessary to analyze the system complete behavior, because electric dynamics can interact with the mechanic vibration dynamics. The electrical circuit that can represent the induction motor is shown in Fig. 2.

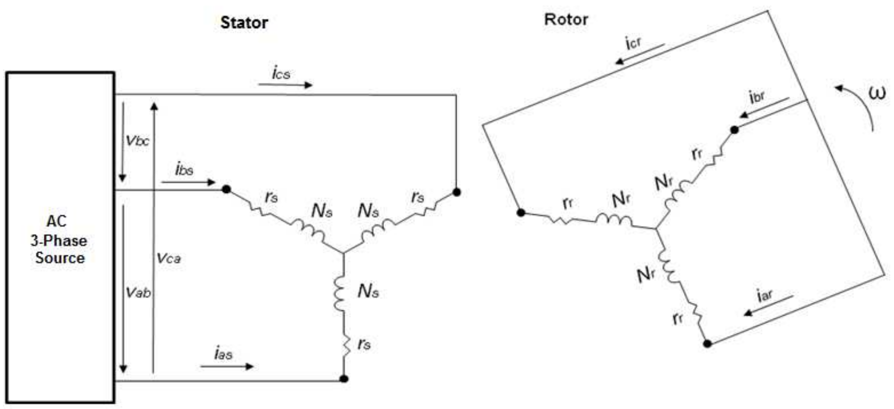

Figure 2. Induction motor electric circuit representation

As can be seen in Krause *et al.* (2002), motor dynamical model can be written in function of motor magnetic flow rates and voltages. If the equations have its referential changed by a referential frame transformation, like Park's or Clark's d-q transformation, the rotor variable position dependence is eliminated and the differential equations coefficient can be written, as constants and the system can be easily simulated. This model can be mathematically expressed according to Eq. 10.

$$\begin{bmatrix} v_{qs} \\ v_{ds} \\ v_{0s} \\ 0 \\ 0 \\ 0 \end{bmatrix} = \begin{bmatrix} a_{11} & a_{12} & 0 & a_{14} & 0 & 0 \\ a_{21} & a_{22} & 0 & 0 & a_{25} & 0 \\ 0 & 0 & a_{33} & 0 & 0 & 0 \\ a_{41} & 0 & 0 & a_{44} & a_{45} & 0 \\ 0 & a_{52} & 0 & a_{54} & a_{55} & 0 \\ 0 & 0 & 0 & 0 & 0 & a_{66} \end{bmatrix} \begin{bmatrix} \psi_{qs} \\ \psi_{ds} \\ \psi_{0s} \\ \psi'_{qr} \\ \psi'_{dr} \\ \psi'_{0r} \end{bmatrix} \tag{10}$$

Where:

$$
\begin{aligned}
& a_{11} = a_{22} = \frac{r_s X'_{rr}}{D} + \frac{1}{\omega_b}\frac{d}{dt} \quad a_{12} = -a_{21} = \frac{\omega}{\omega_b} \\
& a_{14} = a_{25} = -\frac{r_s X_M}{D} \qquad a_{33} = \frac{r_s}{X_{ls}} + \frac{1}{\omega_b}\frac{d}{dt} \\
& a_{41} = a_{52} = -\frac{r'_r X_M}{D} \qquad a_{44} = a_{55} = \frac{r'_r X_{ss}}{D} + \frac{1}{\omega_b}\frac{d}{dt} \\
& a_{45} = -a_{54} = \frac{\omega - \omega_r}{\omega_b} \qquad a_{66} = \frac{r'_r}{X'_{lr}} + \frac{1}{\omega_b}\frac{d}{dt}
\end{aligned}
\tag{11}
$$

In Eq. 11, X_{ss}, X'_{rr} and D parameters are another parameters functions, as follows:

$$
\begin{aligned}
& X_{ss} = X_{ls} + X_M \\
& X'_{rr} = X'_{lr} + X_M \\
& D = X_{ss} X'_{rr} - X_M{}^2
\end{aligned}
\tag{12}
$$

Moreover, T_e torque can be written as:

$$
T_e = \left(\frac{3}{2}\right)\left(\frac{P}{2}\right)\left(\frac{X_M}{D\omega_b}\right)\left(\psi_{qs}\psi'_{dr} - \psi'_{qr}\psi_{ds}\right) \tag{13}
$$

3.3 Space State Model

In order to prepare the simulation complete model, it is necessary to rewrite the dynamic equations in space state. Then, Eq. (8) and Eq. (9) are rewritten as:

$$
\ddot{x} = \frac{-1}{\left(1 - \mu\varepsilon\sin^2\theta\right)}\left[\zeta_x\dot{x} + \omega_0^2 x + \mu\sin\theta\zeta_\theta\dot{\theta} + \mu\varepsilon g\frac{\sin 2\theta}{2} - \mu\sin\theta\zeta_\theta\alpha T + \mu sen\theta\alpha T_L - \mu\cos\theta\dot{\theta}^2\right] \tag{14}
$$

$$
\ddot{\theta} = \frac{-1}{\left(1 - \mu\varepsilon\sin^2\theta\right)}\left[\zeta_\theta\dot{\theta} + \varepsilon\sin\theta\zeta_x\dot{x} + \varepsilon\omega_0^2\sin\theta x + \mu\varepsilon\frac{\sin 2\theta}{2}\dot{\theta}^2 + \varepsilon g\cos\theta - \alpha T_e + \alpha T_L\right] \tag{15}
$$

State space variables can be defines as follows:

$$
\begin{aligned}
& x_1 = \Psi_{qs} \qquad x_3 = \Psi'_{qr} \qquad x_5 = x \qquad x_7 = \theta \\
& x_2 = \Psi_{ds} \qquad x_4 = \Psi'_{ds} \qquad x_6 = \dot{x} \qquad x_8 = \dot{\theta}
\end{aligned}
\tag{16}
$$

The complete space state equations that represent the system complete dynamic model can be now condensed in Eq. 17, where ω_r (see Eq. 11) was replaced by $\frac{\dot{\theta}\cdot P}{2}$ (P is the motor number of poles), as frame reference was fixed, for electrical dynamics analysis, in the motor rotor.

With this model, the complete system can be simulated.

$$
\dot{x}_1 = \dot{\psi}_{qs} = \omega_b\left[v_{qs} - \frac{r_s X'_{rr}}{D}\psi_{qs} - \frac{\omega}{\omega_b}\psi_{ds} + \frac{r_s X_M}{D}\psi'_{qr}\right] \tag{17-a}
$$

$$
\dot{x}_2 = \dot{\psi}_{ds} = \omega_b\left[v_{ds} - \frac{r_s X'_{rr}}{D}\psi_{ds} + \frac{\omega}{\omega_b}\psi_{qs} + \frac{r_s X_M}{D}\psi'_{dr}\right] \tag{17-b}
$$

$$\dot{x}_3 = \dot{\psi}'_{qr} = \omega_b \left[-\frac{r'_r X_{ss}}{D}\psi'_{qr} - \frac{\left(\omega - \dot{\theta}\frac{P}{2}\right)}{\omega_b}\psi'_{dr} + \frac{r'_r X_M}{D}\psi_{qs} \right] \tag{17-c}$$

$$\dot{x}_4 = \dot{\psi}'_{dr} = \omega_b \left[-\frac{r'_r X_{ss}}{D}\psi'_{dr} + \frac{\left(\omega - \dot{\theta}\frac{P}{2}\right)}{\omega_b}\psi'_{qr} + \frac{r'_r X_M}{D}\psi_{ds} \right] \tag{17-d}$$

$$\dot{x}_5 = x_6 = \dot{x} \tag{17-e}$$

$$\dot{x}_6 = \ddot{x} = \frac{-1}{\left(1-\mu\varepsilon\sin^2\theta\right)}\left[\zeta_x\dot{x} + \omega_0^2 x + \mu\sin\theta\zeta_\theta\dot{\theta} + \mu\varepsilon g\frac{\sin 2\theta}{2} - \mu\sin\theta\zeta_\theta\alpha T_e + \mu\sin\theta\alpha T_L - \mu\cos\theta\dot{\theta}^2\right] \tag{17-f}$$

$$\dot{x}_7 = x_8 = \dot{\theta} \tag{17-g}$$

$$\dot{x}_8 = \ddot{\theta} = \frac{-1}{\left(1-\mu\varepsilon\sin^2\theta\right)}\left[\zeta_\theta\dot{\theta} + \varepsilon\sin\theta\zeta_x\dot{x} + \varepsilon\omega_0^2\sin\theta x + \mu\varepsilon\frac{\sin 2\theta}{2}\dot{\theta}^2 + \varepsilon g\cos\theta - \alpha T_e + \alpha T_L\right] \tag{17-h}$$

3.4 Simulation and Results

Two simulation types have been processed, one to simulate TIM direct start and another to simulate the start using a frequency inverter. Motor and mechanical parameters are listed in Table 1.

Table 1. Simulation of Mechanical and Electrical Parameters.

Electrical parameters		**Mechanical parameters**	
Parameter	**Value**	**Parameter**	**Value**
R_s	0.19 Ω	c_θ	0.001 N.m.s/rad
R_r	0.07 Ω	c_x	10 N.s/m
X_{lr}	0.38 Ω	J	0.001 kg.m²
X_{ls}	0.75 Ω	r	0.005 m
X_m	20 Ω	M	5 kg
P	4	g	10 m/s²
		κ	0

The system was simulated with Matlab/Simulink™ software. Natural resonance speed was adjusted in 140 rad/s.

In the direct start simulation, the unbalance degree parameter g_d varied from 10e-4 to 200e-4 kg.m, in order to verify the system behavior.

Fig. 3 shows motor speed during a direct start, when the unbalance degree was of 10e-4 kg.m and 200 e-4 kg.m. It is possible to verify that motor speed passed through resonance speed without any perturbation, although oscillation amplitude grew as unbalance degree grew.

This result agrees with systems studied in Leonov (2008), where the author showed that a synchronous AC motor starting like a TIM cannot be captured by Sommerfeld effect.

In order to start through a frequency inverter, the unbalance degree varied from 10e-4 kg.m to 300 e-4 kg.m, to stress the system and verify if oscillation problems can occur.

TIM start simulation strategy was of stair mode, like ESP (Electric Submergible Pump) in petroleum wells, in order to simulate a quasi-static situation. Results for three different unbalance degrees are presented in Fig. 4 and Fig. 5.

In order to verify nonlinear effects presence in the motor speed, two other analyzes were made, one to verify the resonance region speed oscillation frequency spectrum and another to check the linearity between inverter speed reference and motor medium speed during the start in steps.

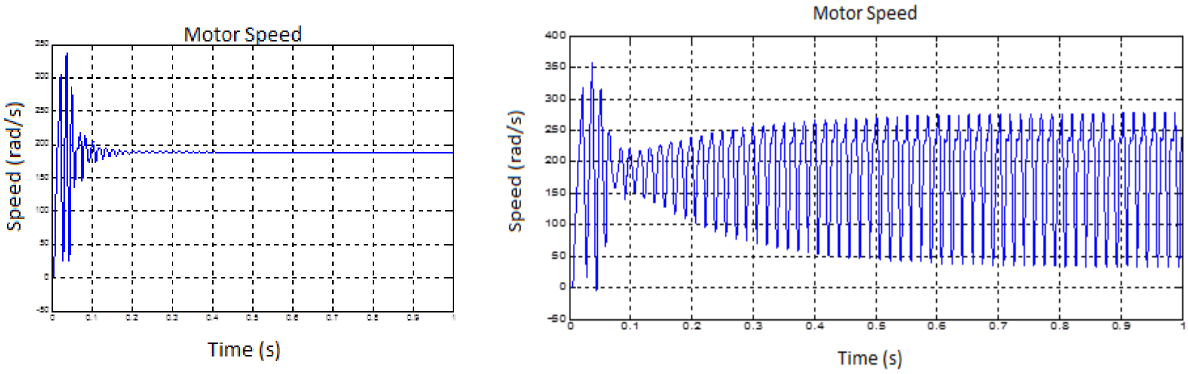

Figure 3. Motor speed during a direct start with unbalance degree of 10e-4 kg.m and 200 e-4 kg.m.

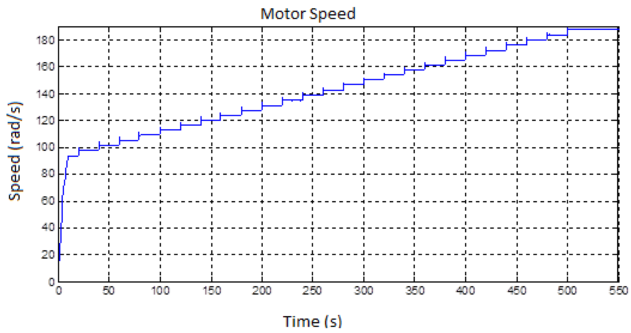

Figure. 4. Motor speed during a frequency inverter start with unbalance degree of 10e-4 kg.m.

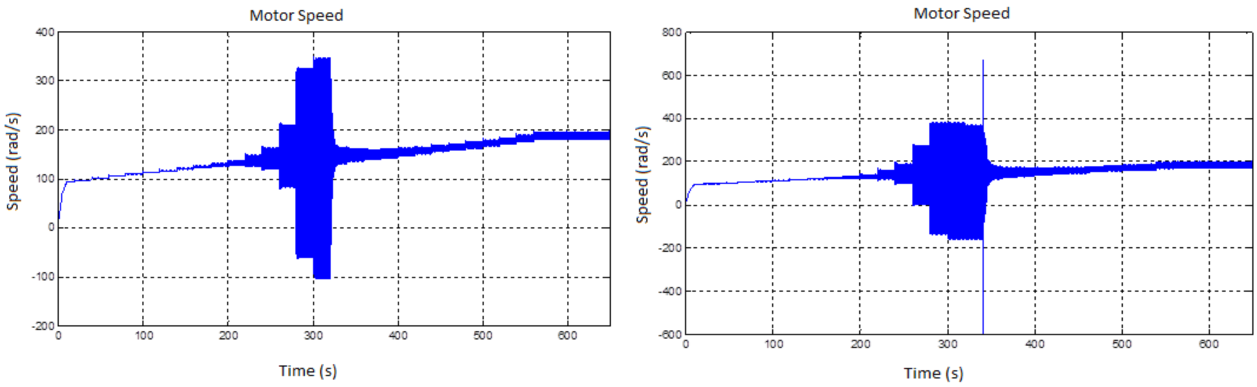

Figure 5. Motor speed during a frequency inverter start with unbalance degree of 200e-4 kg.m and 300e-4 kg.m.

The frequency analysis was made with FFT (Fast Fourrier Transform) technique, with a sample of the speed oscillation in the resonance region.

Frequency analysis results are show in Fig. 6 and Fig. 7.

Linearity analysis was made comparing the speed reference for the inverter, as input, and the motor medium speed for each step during the start. Results are show in Fig. 8 and Fig. 9.

3.5 Simulation Results Comments

As can be seen in Fig. 9, there are evidences that indicate nonlinearity presence on the input-output relation for unbalance degree larger values. It is possible to say that it is Sommerfeld effect evidence in TIM starts with a frequency inverter, even without nonlinear coil or damping, unlike showed Zucovic and Cveticanin (2009).

Chaotic movements existence is always possible in nonlinear systems. With increasing unbalance degree, motor shaft rotation variation, primary motor bracket excitation, increases substantially, and even show reversal signs, although in the short time span (see Fig. 5). This shows rotation axis high instability and, therefore, high instability of its own primary support excitation, which is indicative of a lack of predictability deterministic response, the exact qualitative chaos characteristic.

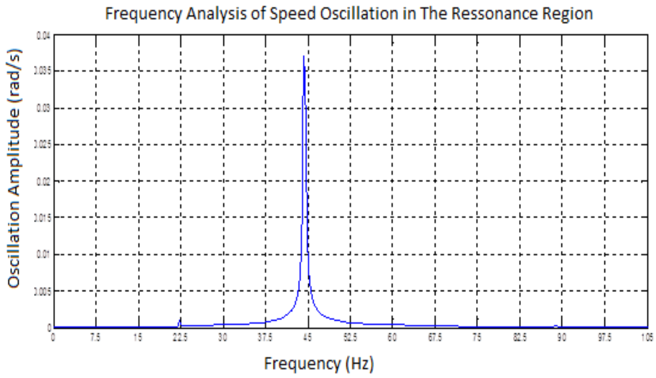

Figure. 6. Resonance region oscillation speed frequency analysis of 10e-4 kg.m unbalance degree.

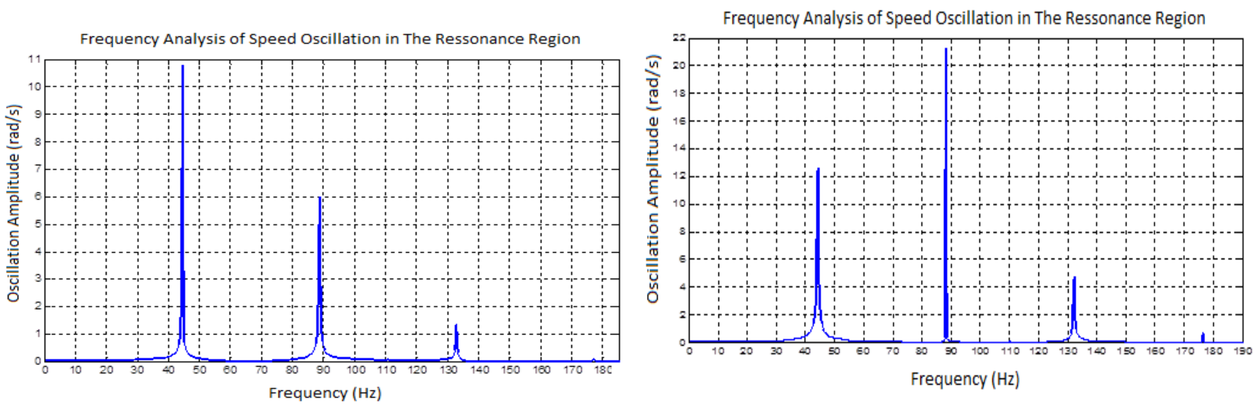

Figure 7. Resonance region oscillation speed frequency analysis of 200e-4 kg.m and 300e-4 kg.m unbalance degree.

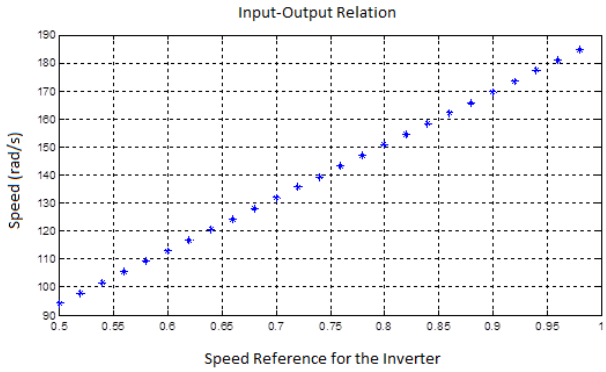

Figure. 8. 10e-4 kg.m unbalance degree Input-Output analysis.

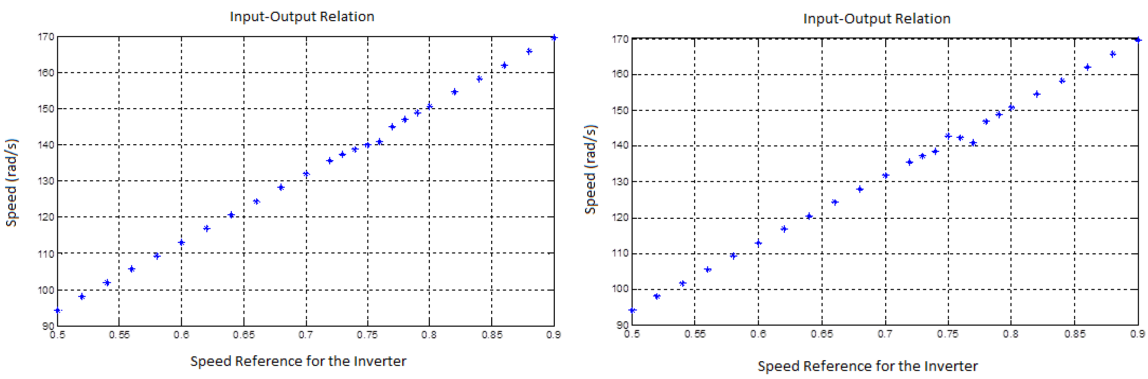

Figure. 9. 200e-4 kg.m and 300e-4 kg.m unbalance degree Input-Output analysis.

It can be observed to some unbalance degree that the response spectrum shows that various frequencies shall play relevant role in the response, rather than one dominating the response. The frequency spectrum scattering, where the main excitement does not change (in this case, the motor drive), is a classic indication of the system dynamics complexity, which may lead to chaos.

Besides the scattering spectrum, it is noted that it occurs at frequencies that are related to the system natural frequency, showing energy flow between natural dynamics and forced dynamics, what points to a kind of "two dynamic competition", which generates response unpredictability, indicative of the chaos possibility.

Finally, it is noted that frequencies that are multiple and sub-multiple of the natural frequency emergence is a classic route to chaos, inside what is called a doubling bifurcation period (sub-multiple frequency) or frequency doubling (multiple frequencies). In both cases, the bifurcation diagram (or the Poincaré map, if applicable) will enter a response in future uncertainty route periods.

3.6 Conclusion

In this work, a mechanical system composed of a three phase AC induction motor and its elastic foundation has been studied.

Dynamic equations were used to get a complete model, which was not found in any other study in the literature. In part, this is due to the three-phase induction motor dynamic behavior complexity. Electrical engineering deals with electrical interactions very specific characteristics, leaving aside the possible influences of mechanical order disturbances. In turn, mechanical engineering does not usually take into account electrical order disturbances influences in the mechanical system dynamics study. As a result of this study, an integrated model that can be applied in many detailed studies on the possibility of very particular movements was done, as already observed in several nonideal system studies.

A complete analysis of the possible answers that the system can provide was not done. The idea was to develop a model and show with reasonable simulations set that this system may have irregular movements, such as those resulting from Sommerfeld effect, i.e. the motor part rotational movement “capture” dictated by electricity dynamics and the mechanical oscillator natural frequency.

Simulations aimed to observe vibration influence on the motor-elastic base set speed passage through resonance and motor speed Sommerfeld effect check, as also sought Leonov (2008) and Zucovic and Cveticanin (2009), were performed with simplified motor models scan. Simulations were performed in Matlab ™.

Two types of motor accelerations were simulated: direct start and starting ramp with frequency inverter. As can be seen in Fig. 3, for direct starting, even passing through the resonance region, no nonlinear oscillatory effect was observed during motor acceleration, as demonstrated analytically in system simplified model in Leonov (2008).

For acceleration ramp, through simulating a start in steps with the frequency inverter, approaching the resonance region, speed fluctuation in speed increased considerably as the imbalance degree grew, and input-output relation discontinuity was observed for an unbalance degree equal to 200e-4 kg.m. Furthermore, motor speed spectrum oscillation frequency analysis was taken, as perceiving that as the unbalance degree increases, the more distorted is the waveform characteristic of the system response, moving away from linear response.

These system types model is fully developed, which takes into account all electric machine dynamics and its interaction with mechanical dynamics. As shown, there is Sommerfeld effect and chaos route presence indication and it is important to know and prevent these effects for correct system performance.

4. REFERENCES

Balthazar, J. M, Mook D. T, Weber, H. I, Reyolando, M. L. R. F, Fenili, A, Belato, D, Feliz J. L. P., 2003. "An overview on non- ideal vibrations". Meccanica. 7p.

Krause, P. C., Wasynczuk, O., Sudhoff, S., 2002. "Analysis of Electric Machinary and Drive Systems" 2º Ed. IEEE Press, 630p.

Leonov, G. A., 2008. "The Passage Through Resonance of Synchronous Electric Motors Mounted on an Elastic Base", Journal of Applied Mathematics and Mechanics n.72, pp 631-637.

Rao, S. R. "Mechanical Vibration" 424p, Pearson Prentice Hall, 2008.

Rocha Júnior, E. B., 2004. "Análise da dinâmica acoplada de uma máquina elétrica rotativa e sua estrutura de suporte". Dissertação de Mestrado, Universidade Federal do Espírito Santo, 85p.

Strogatz, S. H., 1994. "Nonlinear Dynamics and Chaos", 420p, Westview.

Zukovic, M. and Cveticanin, L., 2009. "Chaos in Non Ideal Mechanical System with Clearence". Journal of Vibration and Control. 2009.